Introduction to X-ray Absorption Spectroscopy

Bruce Ravel
Synchrotron Science Group
National Institute of Standards and Technology
&
Beamline for Materials Measurements
National Synchrotron Light Source II

XAS 2023: Fundamentals of XAS Data Analysis: A Hands-on Tutorial

10 October, 2023

Part 1

The basic physics and chemistry of X-ray Absorption

This Talk

This talk is an introduction to the inner-shell spectroscopies, XAS and XRF.

Outline

- An overview of the basic physics of inner shell spectroscopies
- An introduction to XAS and XRF beamline instrumentation
- A flavor of the sorts of science that can be accomplished with XAS and XRF, including examples from my own research and my beamline.

My hope is that you will leave with a sense of how XAS and XRF might be applied to your research.

XAS and XRF

X-ray Absorption Spectroscopy
and
X-Ray Fluorescence spectroscopy

These are inner shell spectroscopies.

Inner shell means that an x-ray interacts primarily with a deep-core electron rather than with a valence electron.

Spectroscopy means that some aspect of the interaction changes as a function of photon energy.

XAS and XRF

X-ray Absorption Spectroscopy
and
X-Ray Fluorescence spectroscopy

These are inner shell spectroscopies.

Inner shell means that an x-ray interacts primarily with a deep-core electron rather than with a valence electron.

Spectroscopy means that some aspect of the interaction changes as a function of photon energy.

XAS and XRF

X-ray Absorption Spectroscopy
and
X-Ray Fluorescence spectroscopy

These are inner shell spectroscopies.

Inner shell means that an x-ray interacts primarily with a deep-core electron rather than with a valence electron.

Spectroscopy means that some aspect of the interaction changes as a function of photon energy.

The basic physical process in XAS and XRF

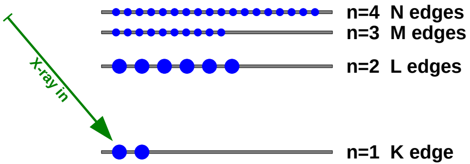

1. An incoming photon interacts with a deep-core electron. Shown here, a 1s electron is excited for a K-edge spectrum.
2. The deep-core electron is promoted to some unoccupied state above the Fermi energy, propagates away, and leaves behind a core-hole.
3. A short time later (1 or 2 femtoseconds), a higher-lying electron decays into the core-hole and emits a photon. Shown here, a $2p^{3/2}$ or $2p^{1/2}$ electron fills the 1s hole.
4. Alternately, the energy from the higher-lying electron can be used to emit an Auger electron.

The basic physical process in XAS and XRF

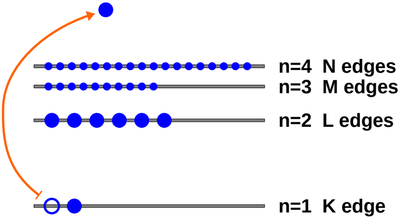

1. An incoming photon interacts with a deep-core electron. Shown here, a 1s electron is excited for a K-edge spectrum.
2. The deep-core electron is promoted to some unoccupied state above the Fermi energy, propagates away, and leaves behind a core-hole.
3. A short time later (1 or 2 femtoseconds), a higher-lying electron decays into the core-hole and emits a photon. Shown here, a $2p^{3/2}$ or $2p^{1/2}$ electron fills the 1s hole.
4. Alternately, the energy from the higher-lying electron can be used to emit an Auger electron.

The basic physical process in XAS and XRF

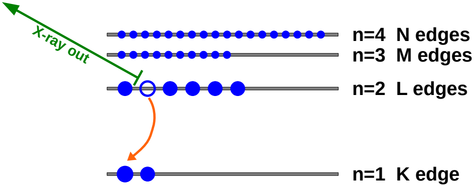

1. An incoming photon interacts with a deep-core electron. Shown here, a 1s electron is excited for a K-edge spectrum.
2. The deep-core electron is promoted to some unoccupied state above the Fermi energy, propagates away, and leaves behind a core-hole.
3. A short time later (1 or 2 femtoseconds), a higher-lying electron decays into the core-hole and emits a photon. Shown here, a $2p^{3/2}$ or $2p^{1/2}$ electron fills the 1s hole.
4. Alternately, the energy from the higher-lying electron can be used to emit an Auger electron.

The basic physical process in XAS and XRF

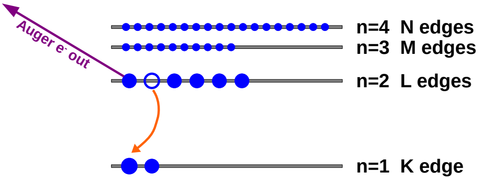

1. An incoming photon interacts with a deep-core electron. Shown here, a 1s electron is excited for a K-edge spectrum.
2. The deep-core electron is promoted to some unoccupied state above the Fermi energy, propagates away, and leaves behind a core-hole.
3. A short time later (1 or 2 femtoseconds), a higher-lying electron decays into the core-hole and emits a photon. Shown here, a $2p^{3/2}$ or $2p^{1/2}$ electron fills the 1s hole.
4. Alternately, the energy from the higher-lying electron can be used to emit an Auger electron.

Elements and Beamlines

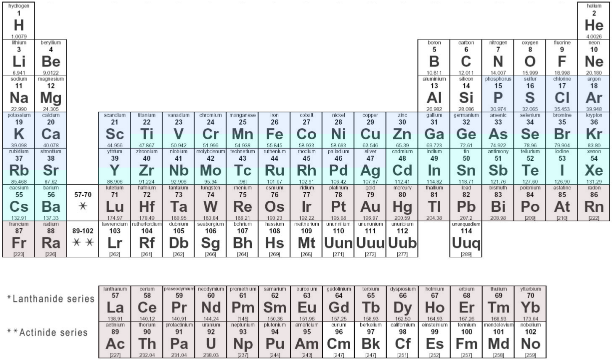

K- or L-edges measured at a soft-X-ray beamline

K-edges measured at a hard-X-ray beamline

L-edges measured at a hard-X-ray beamline

Elements and Beamlines

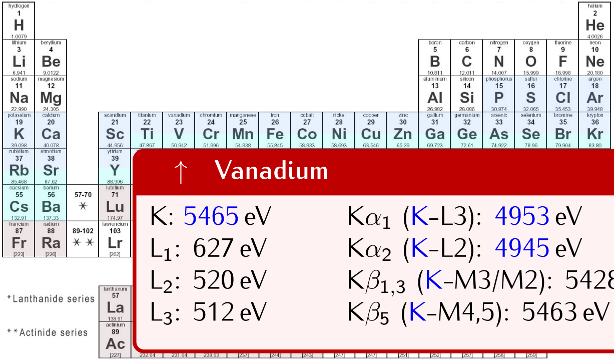

↑ Vanadium

K: 5465 eV	Kα_1 (K-L3): 4953 eV
L_1: 627 eV	Kα_2 (K-L2): 4945 eV
L_2: 520 eV	K$\beta_{1,3}$ (K-M3/M2): 5428 eV
L_3: 512 eV	Kβ_5 (K-M4,5): 5463 eV

K- or L-edges measured at a soft-X-ray beamline

K-edges measured at a hard-X-ray beamline

L-edges measured at a hard-X-ray beamline

Elements and Beamlines

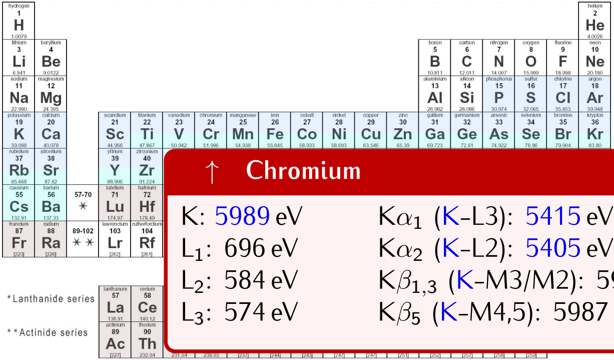

↑ Chromium

K: 5989 eV	$K\alpha_1$ (K-L3): 5415 eV
L_1: 696 eV	$K\alpha_2$ (K-L2): 5405 eV
L_2: 584 eV	$K\beta_{1,3}$ (K-M3/M2): 5947 eV
L_3: 574 eV	$K\beta_5$ (K-M4,5): 5987 eV

K- or L-edges measured at a soft-X-ray beamline

K-edges measured at a hard-X-ray beamline

L-edges measured at a hard-X-ray beamline

Elements and Beamlines

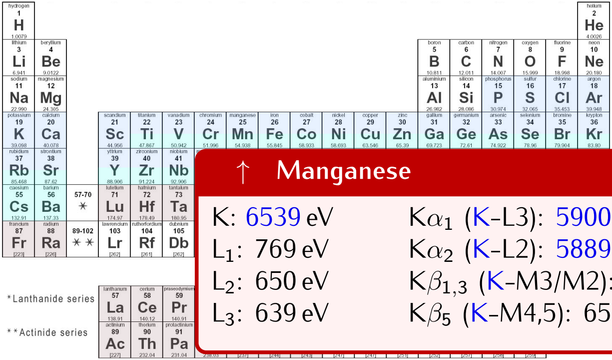

↑ Manganese

K: 6539 eV	$K\alpha_1$ (K-L3): 5900 eV
L_1: 769 eV	$K\alpha_2$ (K-L2): 5889 eV
L_2: 650 eV	$K\beta_{1,3}$ (K-M3/M2): 6492 eV
L_3: 639 eV	$K\beta_5$ (K-M4,5): 6537 eV

K- or L-edges measured at a soft-X-ray beamline

K-edges measured at a hard-X-ray beamline

L-edges measured at a hard-X-ray beamline

Elements and Beamlines

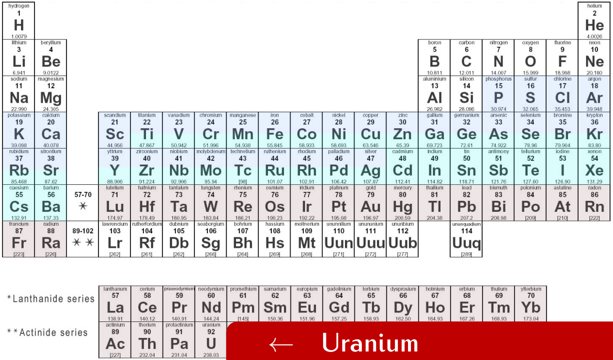

K- or L-edges me

K-edges measu

L-edges measu

← Uranium

K: 115606 eV	$L\alpha_1$ (L3-M5), 13614 eV
L_1: 21757 eV	$L\alpha_2$ (L3-M4), 13438 eV
L_2: 20948 eV	$L\beta_2$ (L3-N4,5), 16388 eV
L_3: 17166 eV	$L\beta_5$ (L3-O4,5), 17063 eV
	$L\beta_6$ (L3-N1): 15727 eV
	L_ℓ (L3-M1): 11618 eV

A simple picture of X-ray absorption

An incident x-ray of energy E is absorbed, destroying a core electron of binding energy E_0 and emitting a photo-electron with kinetic energy $(E - E_0)$. The core state is eventually filled, ejecting a fluorescent x-ray or an Auger electron.

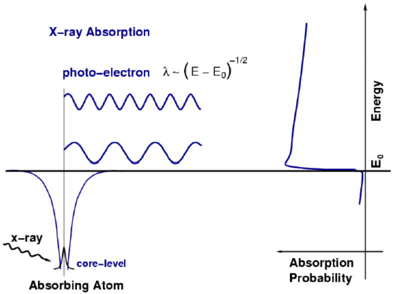

An empty final state is required.
No available state,
no absorption!
When the incident x-ray energy is larger than the binding energy, there is a sharp increase in absorption.

For an isolated atom, $\mu(E)$ has a sharp step at the core-level binding energy and is a smooth function of energy above the edge.

Image from Matt Newville

X-ray absorption in condensed matter

The ejected photo-electron can scatter from neighboring atoms. R has some relationship to λ and there is a phase shift associated with the scattering event. Thus the outgoing and scattered waves interfere.

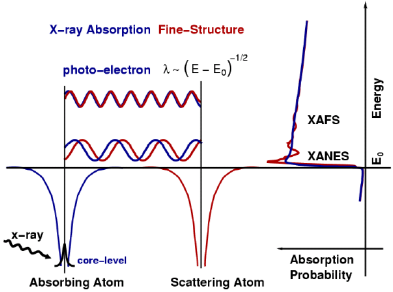

The scattering of the photo-electron wave function interferes with itself.

$\mu(E)$ depends on the density of states with energy $(E - E_0)$ at the absorbing atom.

This interference at the absorbing atom will vary with energy, causing the oscillations in $\mu(E)$.

Image from Matt Newville

XAS and Valence State

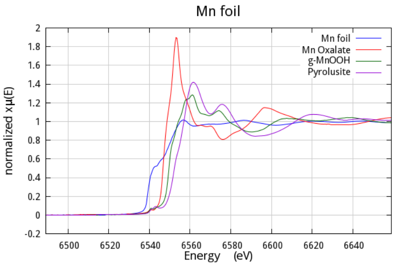

As the valence increases

$Mn^0 \rightarrow Mn^{2+} \rightarrow Mn^{3+} \rightarrow Mn^{4+}$

the edge position shifts to higher energy.

XAS is a direct measure of valence state

- Since each element has its own edge energy, an element's valence can be measured even in a heterogeneous sample
- Since x-rays are deeply penetrating into matter, samples often require only preparation
- No assumption of symmetry or periodicity is made, so the sample can be crystalline, amorphous, thin film, in solution, surface sorbed, $\cdots$, *whatever*

XAS and Local Atomic Structure

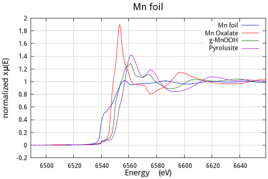

- The different Mn species display big differences in the fine structure beyond the edge as the valence increases (Mn^0, Mn^{2+}, Mn^{3+}, Mn^{4+}). The white line and subsequent oscillations are quite different.
- The oscillatory portion of the spectrum can be isolated and ...
- ... Fourier transformed. This FT function can be interpreted to yield partial pair distribution functions of atoms about the absorber. The Mn-O distances are different for the Mn^{2+}, Mn^{3+}, and Mn^{4+} and clearly different from the Mn-Mn distance in Mn metal.

XAS and Local Atomic Structure

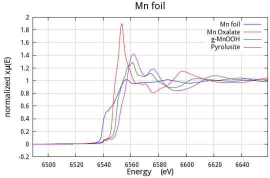

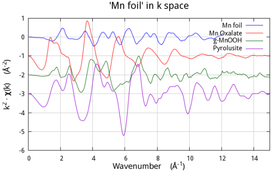

- The different Mn species display big differences in the fine structure beyond the edge as the valence increases (Mn^0, Mn^{2+}, Mn^{3+}, Mn^{4+}). The white line and subsequent oscillations are quite different.
- The oscillatory portion of the spectrum can be isolated and ...
- ... Fourier transformed. This FT function can be interpreted to yield partial pair distribution functions of atoms about the absorber. The Mn-O distances are different for the Mn^{2+}, Mn^{3+}, and Mn^{4+} and clearly different from the Mn-Mn distance in Mn metal.

XAS and Local Atomic Structure

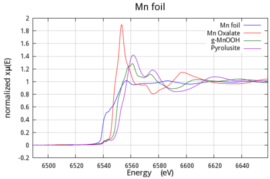

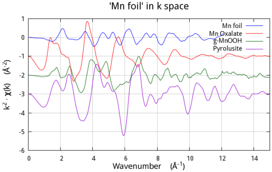

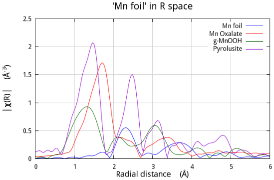

- The different Mn species display big differences in the fine structure beyond the edge as the valence increases (Mn^{0}, Mn^{2+}, Mn^{3+}, Mn^{4+}). The white line and subsequent oscillations are quite different.
- The oscillatory portion of the spectrum can be isolated and ...
- ... Fourier transformed. This FT function can be interpreted to yield partial pair distribution functions of atoms about the absorber. The Mn-O distances are different for the Mn^{2+}, Mn^{3+}, and Mn^{4+} and clearly different from the Mn-Mn distance in Mn metal.

Fluorescence from Many Elements

X-ray fluorescence is a spectroscopy in which the incident energy is fixed and the energy dependence of the secondary photons is measured.

Every element with an edge below the incident energy will fluoresce.

Glass with every 2^{nd} element Ca–Ge, incident energy = 11153 eV

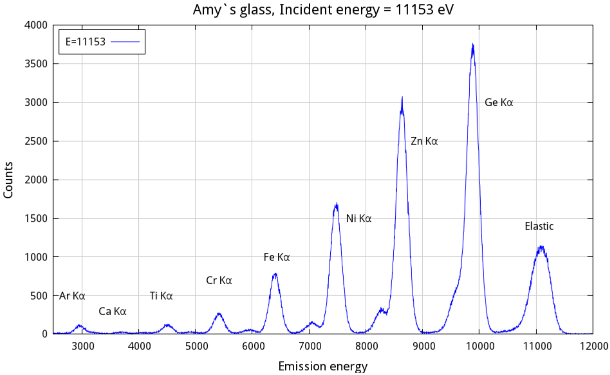

Fluorescence from A Sediment Sample

Here are the XRF spectra with incident beams above and below the U L_{III} edge for a sediment heavily contaminated with uranium.

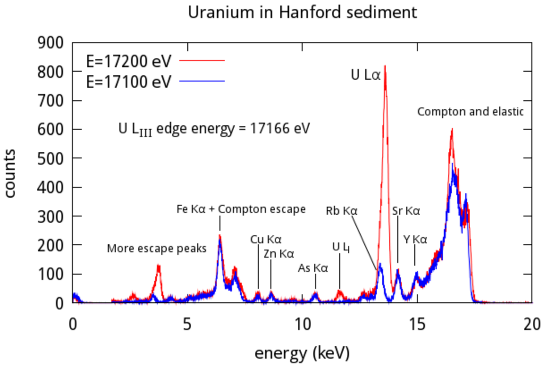

When combined with a standard measured under identical conditions, element concentrations can be *quantified.*

Using the Fluorescence Spectrum for XAS

We can place a region of interest (ROI) around the U Lα peak and measure its variation as a function of incident energy.

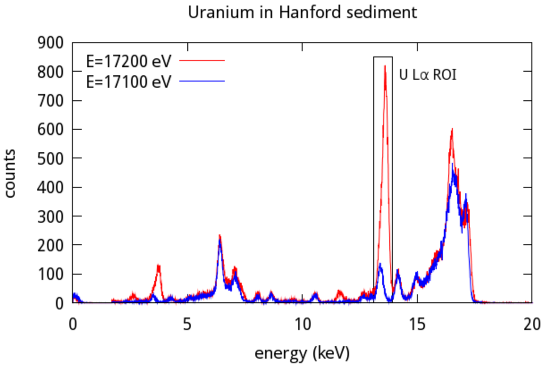

In this way, we measure signal only from the absorber and reject all other photons entering the detector.

Typical optics for an XAS beamline

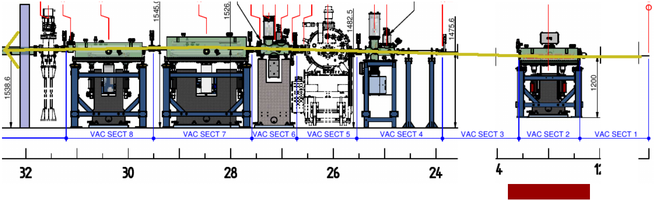

Collimating mirror

Makes the divergent rays from the source parallel, setting the beam size (8 mm × 1 mm at BMM)

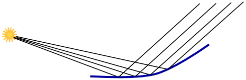

Total external reflection from a paraboloid surface

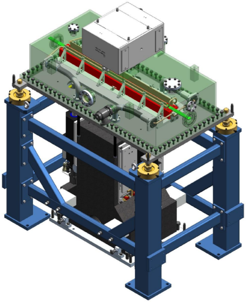

All instrumentation images are from FMB Oxford Beamlines Ltd.

Typical optics for an XAS beamline

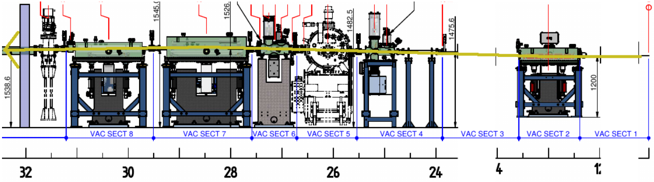

Monochromator

Bragg diffraction from a Si crystal to pass a narrow bandwidth from the pink beam

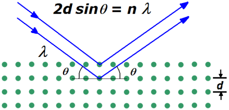

Change energy by changing angle

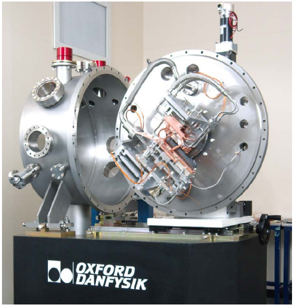

All instrumentation images are from FMB Oxford Beamlines Ltd.

Typical optics for an XAS beamline

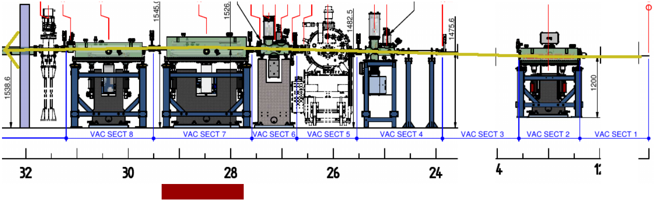

Focusing mirror

Total external reflection from a torroid surface, bent such that rays focus to a spot

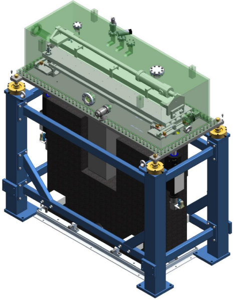

All instrumentation images are from FMB Oxford Beamlines Ltd.
Photo of mirror is from ESRF ID09B

Typical optics for an XAS beamline

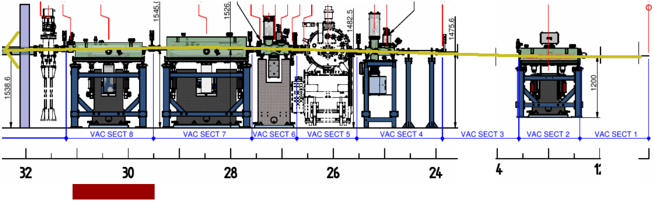

Harmonic rejection mirror

Flat mirror redirects beam from mono and M2

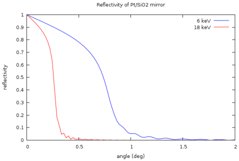

Choose an angle to pass the fundamental but absorb harmonics

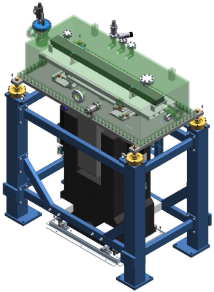

All instrumentation images are from FMB Oxford Beamlines Ltd.

A typical XAS hutch (BMM at NSLS-II)

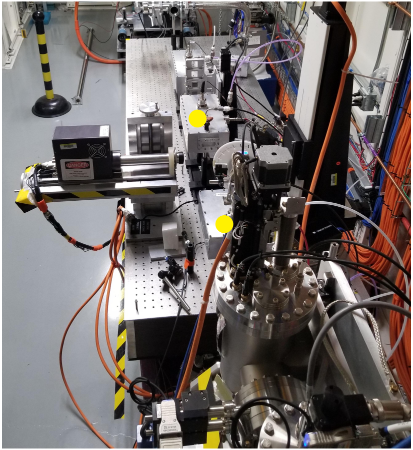

Ionization chambers

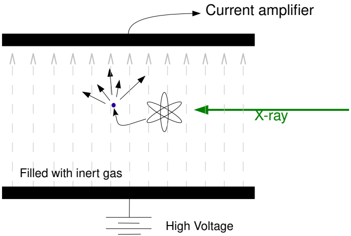

Gas-filled capacitors. Incoming photon ionizes a gas molecule. The electron cascade produces a measurable current.

Transmission XAS

$$\mu(E) = \ln(I_0/I_t)$$

i.e. Beers' Law for X-rays

A typical XAS hutch (BMM at NSLS-II)

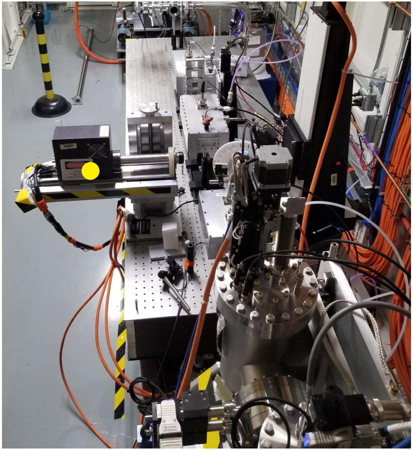

Energy discriminating fluorescence detector

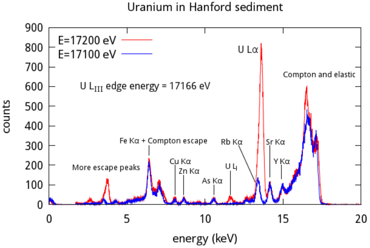

Silicon drift diode measures energy of each photon deposited

Fluorescence XAS

$\mu(E) \propto I_f / I_0$

A typical XAS hutch (BMM at NSLS-II)

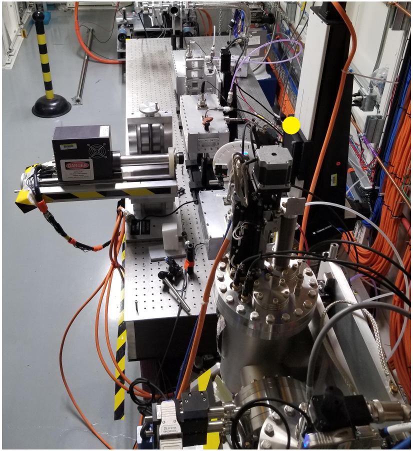

Sample stage

Hard X-rays are deeply penetrating into matter, so the stage could be:

- Cryostat
- Furnace
- Pressure cell
- Electrochemistry cell
- Stop-flow cell
- Gas flow reactor
- Controlled atmosphere

etc. etc. etc.

Real samples under **real** conditions

What is meant by “deeply penetrating”?

The Center for X-ray Optics provides a tool for estimating the attenuation of X-rays as they pass through matter.
http://henke.lbl.gov/optical_constants/atten2.html

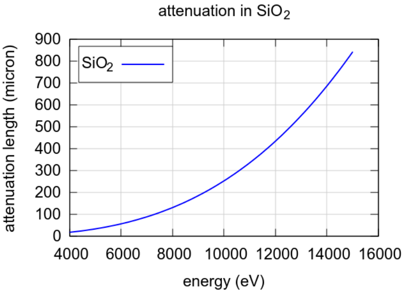

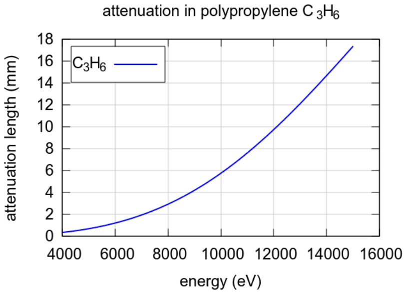

So, windows made of low-Z materials can be quite thick and still pass hard X-rays. This allows deployment of specialized sample environments for use in XAS experiments.

Acronyms

XANES X-ray Absorption Near-Edge Structure

NEXAFS Near-Edge X-ray Absorption Fine Structure

XANES and NEXAFS are exactly the same thing. Historically, the soft X-ray community says “NEXAFS” while the hard X-ray community says “XANES”.

Both acronyms refer to the portion of the XAS (X-ray Absorption Spectroscopy) measurement in the vicinity of the absorption edge.

The Extended X-ray Absorption Fine Structure is oscillatory data extending hundreds of volts above the edge.

Some vocabulary

Words commonly used to describe specific parts of the XANES spectrum.

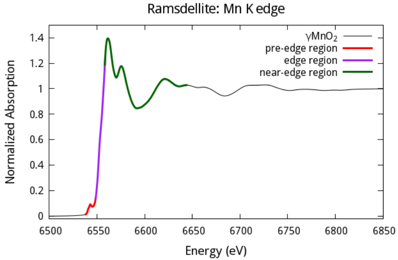

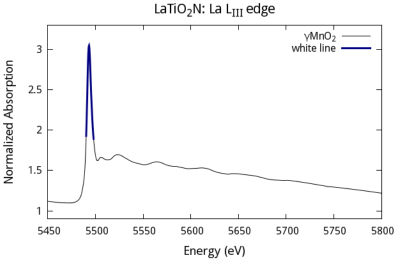

pre-edge Small (or large, certainly meaningful!) features between the Fermi energy and the threshold

edge The main rising part of XAS spectrum

near-edge Characteristic features above the edge

white line Large, prominent peak just above the edge, particularly in L or M edge spectra

Part 2

Understanding XANES

Speciation at a glance: Coordination

Here is Cr K edge data for tetragonally coordinated, hexavalent $K_2C_2r^{VI}O_7$ and hexagonally coordinated, trivalent $Cr_2^{III}O_3$. Trivalent Cr is insoluble and non-toxic. Hexavalent Cr is readily soluble and highly toxic.

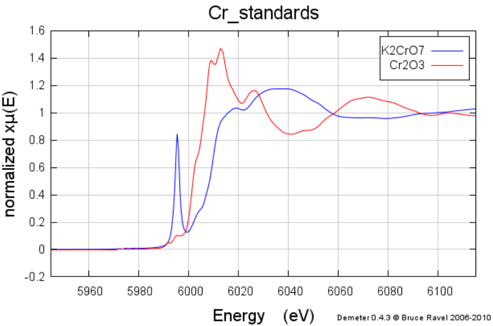

$K_2Cr_2O_7$

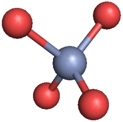

Cr_2O_3

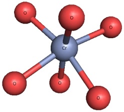

It is very easy to tell “good” Cr from “bad” Cr in a XANES measurement.

data from http://cars9.uchicago.edu/~newville/ModelLib/search.html

Speciation at a glance: Crystallinity

SiO_2 is found in two forms* under standard conditions: crystalline (the mineral quartz) and amorphous (common glass).

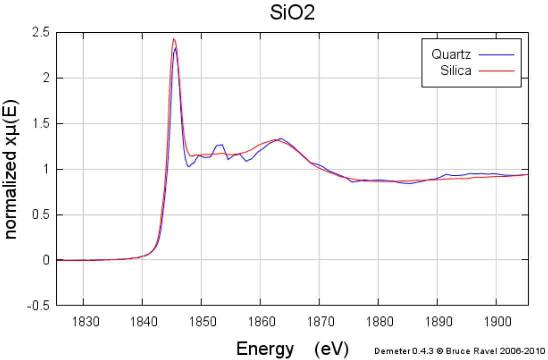

Again, these are readily distinguished by a XANES measurement.

* Wikipedia identifies 14 other metastable, high-T, or high-P forms of SiO_2.

Speciation at a glance: Oxidation

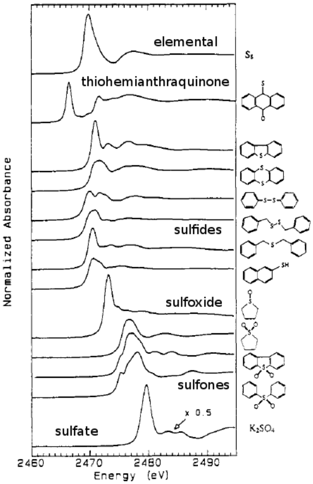

- There is an 11 eV shift from S^{2-} to S^{6+} with lots of variation among species.
- S speciation is of importance across a broad range of disciplines, including life science, catalysis, petroleum science, photovoltaics, environmental science and more.
- P and Cl are similarly rich in their XAS.

Sulfur K-edge x-ray absorption spectroscopy of petroleum asphaltenes and model compounds, G.N. George, M.L. Gorbaty, J. Am. Chem. Soc. (1989) **111**:9, 3182 DOI: 10.1021/ja00191a012

Oxidation and edge position

There is a relationship between formal valence of a metal and the position of the edge in the XANES spectrum. Here is Re metal along with 4+, 6+, and 7+ oxides of Re.

The shift to higher energy is, to first order, a Coulomb effect. Less charge on the atom means less screening of the core.

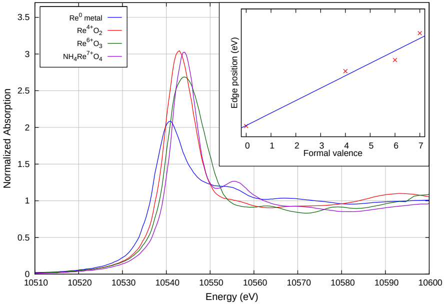

Some more examples:

Mo S.P. Cramer et al. J. Am. Chem. Soc., **98**:5, pp 1287 (1976) DOI: 10.1021/ja00421a053

V J. Wong et al. Phys. Rev. B**30**, 5596–5610 (1984) DOI: 10.1103/PhysRevB.30.5596

Simultaneous XAFS measurements of multiple samples, B. Ravel, C. Scorzato, D.P. Siddons, S.D. Kelly and S.R. Bare, J. Synchrotron Rad. (2010) **17**, 380-385 DOI: 10.1107/S0909049510006230

Mixed phases

Here we see trivalent V_2O_3, pentavalent V_2O_5 and an unknown Vanadium compound plotted together.

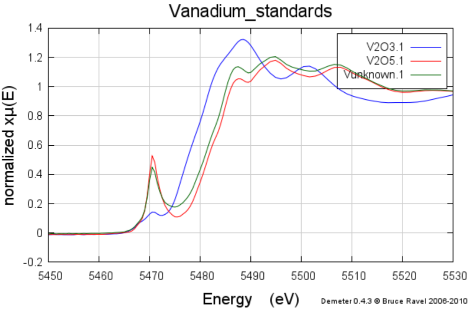

Like in the Cr example, we see a distinct difference between 6-coordinated and 4-coordinated V.

Our unknown is partially reduced, as can be seen by the reduction in pre-edge peak and the left-ward shift of the main edge.

Later we will discuss ways of determining the content of the unknown.

Evolution of redox state

The edge features are often large enough that their evolution can be measured in an *in situ* experiment.

Here we see the kinetics of $Cr^{III} \rightarrow Cr^{VI}$ oxidation by Mn oxide over the course of four minutes of reaction time. Each scan was measured in 3 second.

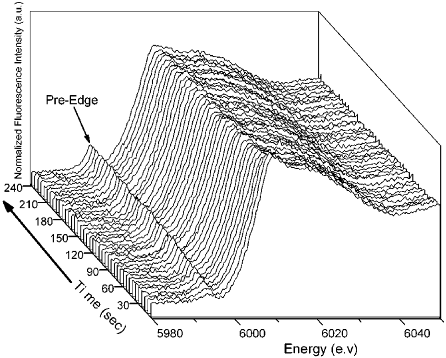

The *in situ* experiment could involve a chemical reaction, a change in temperature, electrochemical cycling, and so on.

Kinetics of Chromium(III) Oxidation by Manganese(IV) Oxides Using Quick Scanning X-ray Absorption Fine Structure Spectroscopy (Q-XAFS), G. Landrot, M. Ginder-Vogel, and D.L. Sparks, Environ. Sci. Technol., (2010) **44**:1, pp 143-149
DOI: 10.1021/es901759w

Ligands

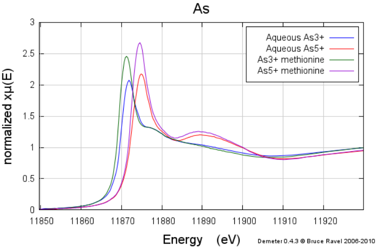

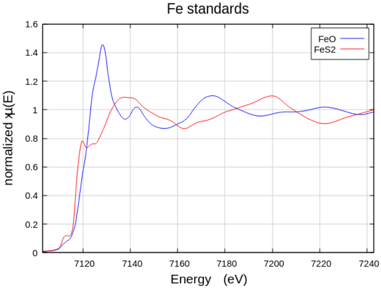

We see a significant edge shift between aqueous As^{3+} and aqueous As^{5+}, as we expect. Note that the As^{3+} and As^{5+} methionine solutions are similar, but shifted to lower energy.

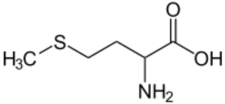

The same shift is seen between divalent wüstite (FeO) and divalent pyrite (FeS_2).

Fingerprinting

Fingerprint, *tr.v.*

To identify by means of a distinctive mark or characteristic.

One of the most powerful uses of XANES data is to simply identify what is in front of the beam.

Looking back at the Cr^{III}/Cr^{VI} example, what might you say about the valence of the chromium contained in coal combustion residue?

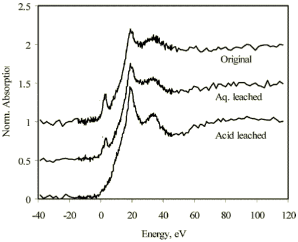

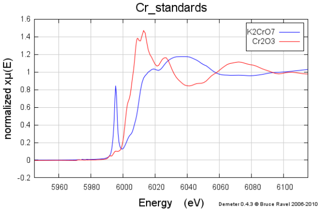

K_2CrO_7

Cr_2O_3

Quantifying Hazardous Species in Particulate Matter Derived from Fossil-Fuel Combustion, F.E. Huggins, et al., Environ. Sci. Technol. (2004) **38**:6, 1836 DOI: 10.1021/es0348748

Categorizing spectra

In an study of Ti-containing standard materials, the different coordination environments were found to aggregate when plotting pre-edge peak height v. peak position.

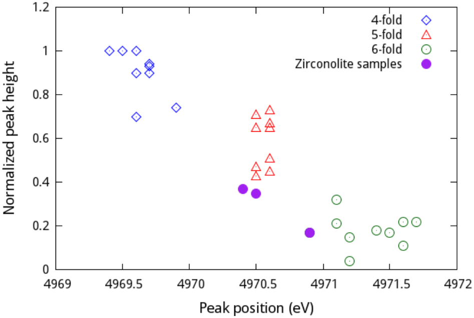

Here we see the data from the reference below along with Ti K-edge data from various Zirconolite ($CaZrTi_2O_7$) samples.

F. Farges, G.E. Brown Jr., J.J. Rehr, *Coordination chemistry of Ti (IV) in silicate glasses and melts: I. XAFS study of titanium coordination in oxide model compounds* , Geochim. Cosmochim/ Acta, **60**:16, 3023, 1996, DOI: 10.1016/0016-7037(96)00144-5

XANES and disorder

The details of the XANES can often give information about structural disorder about the absorbing atom.

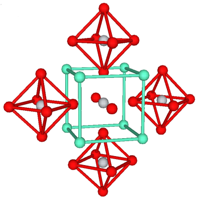

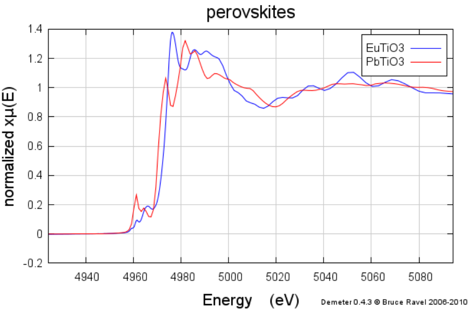

$EuTiO_3$ is a true cubic perovskite. $PbTiO_3$ is a tetragonally distorted perovskite with substantial disorder in the oxygen octahedron. Consequently, the pre-edge peak is much larger for $PbTiO_3$.

B. Ravel, E. A. Stern, R. I. Vedrinskii, V. Kraizman, *Local structure and the phase transitions of* $BaTiO_3$ Ferroelectrics, **206**:1 (1998) 407,
DOI: 10.1080/00150199808009173

Why are local disorder and the pre-edge peak related?

- XAS is a dipole transition. The photoelectron changes angular momentum by 1: $\ell \pm 1$.
- For a K-edge spectrum, the initial state is *s*: $\ell = 0$. Thus the final state must be $\ell = 1$.
- Ti has a filled *p* shell but a completely empty *d* shell.
- With centro-symmetry, as in a true perovskite, the *p* and *d* states cannot hybridize. Broken symmetry leads to mixing of *p* and *d* states around the Fermi level.
- Disorder-driven admixture of *d* character results in an enhanced pre-edge peak.

Analysis

There are a number of ways to get quantitative results from XANES spectra. Here's an incomplete list:

Linear Combination Fitting
: Interpret data by comparison with standards

Peak Fitting
: Fit peak-like and step-like line-shapes to the XANES data

Principle Components Analysis
: Decompose an ensemble of data into a mathematical basis

Difference Spectra
: Subtract one normalized spectrum from another

LCF

The working assumption of LCF

The spectrum from an unknown sample can be understood as a linear superposition of the spectra of two or more known samples.

That is:

+

=

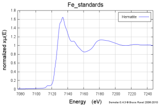

+

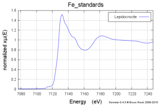

Economic geology (I)

One way that gold deposits form is by having Au chloride fluids rise from the deep earth, wash over cyanobacteria colonies, and reduce to metallic gold.

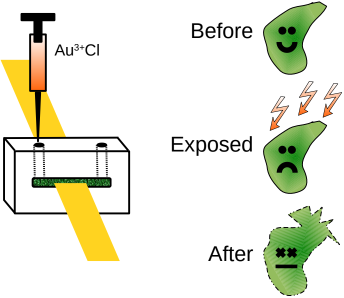

We simulated this process at the beamline by exposing cyanobacteria to an Au^{3+} solution and “watching” the evolution of the Au XAS from Au^{3+} to Au^{0}.

Questions

- What is the rate constant?
- Is there an intermediate species?

M. Lengke et el., *Mechanisms of Gold Bioaccumulation by Filamentous Cyanobacteria from Gold(III)-Chloride Complex*, Environ. Sci. Technol. **40**(20) p. 6304-6309. (2006) DOI: 10.1021/es061040r

Economic geology (II)

We see that 7 minutes after injection, the data strongly resemble the $Au^{3+}Cl$. After one week, the data resemble Au metal.

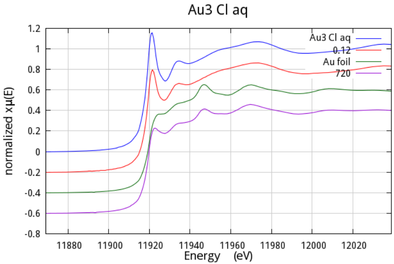

Over the course of the time series, the white line ∼ 11921 shrinks while the bump ∼ 11945 grows, suggesting the reduction to Au metal.

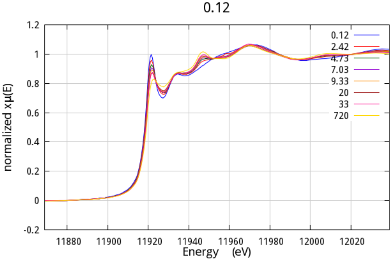

M. Lengke et el., *Mechanisms of Gold Bioaccumulation by Filamentous Cyanobacteria from Gold(III)-Chloride Complex*, Environ. Sci. Technol. **40**(20) p. 6304-6309. (2006) DOI: 10.1021/es061040r

Economic geology (III)

We can analyze these data as a linear combination of species, including $Au^{3+}Cl$, Au metal, and Au^{1+} sulfide.

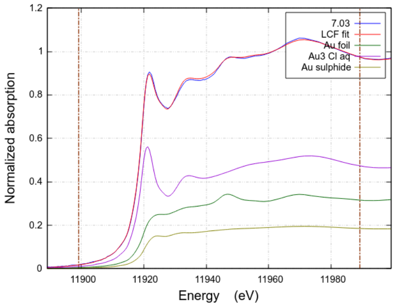

We can plot out the contributions from these species as a function of time to get a sense of reaction rates.

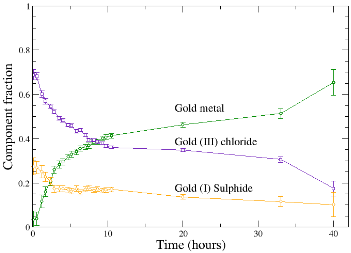

M. Lengke et el., *Mechanisms of Gold Bioaccumulation by Filamentous Cyanobacteria from Gold(III)-Chloride Complex*, Environ. Sci. Technol. **40**(20) p. 6304-6309. (2006) DOI: 10.1021/es061040r

Peak fitting

The working assumption of peak fitting

A spectrum can be meaningfully deconstructed into a set of step-like (atan or erfc) and peak (Gaussian, Lorentzian, Voight) functions.

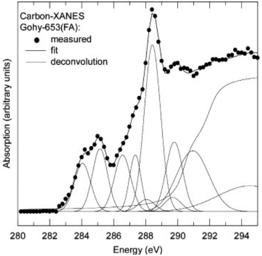

In this case, various Gaussians are interpreted as the main 1s-π^* or Rydberg/mixed valence transitions and two higher energy (1s-2π^*) transition in the C K-edge XANES of a sediment.

This sort of analysis is most meaningful when performed across an ensemble of related data. The drawback is that the physical significance of the line-shapes is sketchy, at best.

T. Schäfer, et al., Organic Geochemistry, 36:4, (2005) 567, DOI: 10.1016/j.orggeochem.2004.10.011

XANES: Principle Components Analysis

PCA is a bit of linear algebra which breaks down an ensemble of related data into abstract components.

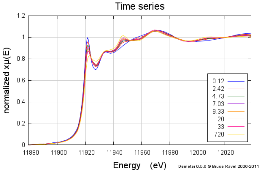

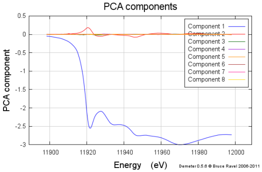

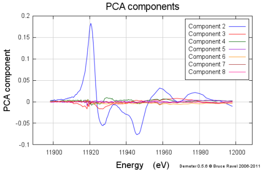

The components can then be used to try to construct a standard as a test to see whether that standard is present in the ensemble.

The number of species represented in the ensemble is related to the number of statistically significant components.

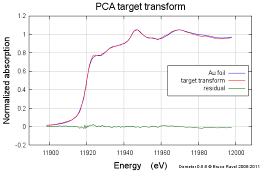

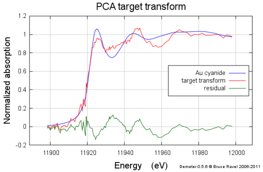

S.R. Wasserman, J. Phys. IV France (1997) C2-203-C2-205; DOI: 10.1051/jp4/1997163
S.R. Wasserman et al., J. Synchrotron Rad. (1999) 6, 284-286; DOI: 10.1107/S0909049599000965
+ references therein

Difference Spectra

Difference spectra

Subtract one spectrum from another.

The most common use is for X-ray Magnetic Circular Dichroism (XMCD)

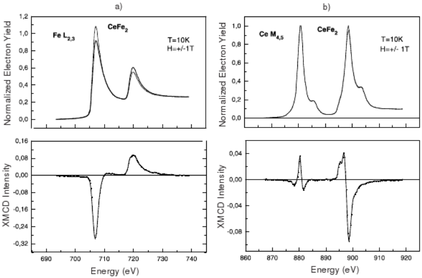

The areas under the difference spectra tell you about moment and magnetic ordering.

Difference spectra can also be used to highlight a subtle change in a data sequence.

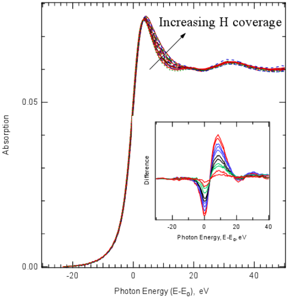

Here, hydogenation of the Pt nanoparticles alters the Pt DOS

X-ray magnetic circular dichroism study on CeFe2, A. Delobbe, et al., Europhys. Lett. 43 320 (1998), DOI: 10.1209/epl/i1998-00359-2
Pt data courtesy of Simon Bare

Part 3

Understanding EXAFS

A simple picture of X-ray absorption

An incident x-ray of energy E is absorbed, destroying a core electron of binding energy E_0 and emitting a photo-electron with kinetic energy $(E - E_0)$. The core state is eventually filled, ejecting a fluorescent x-ray or an Auger electron.

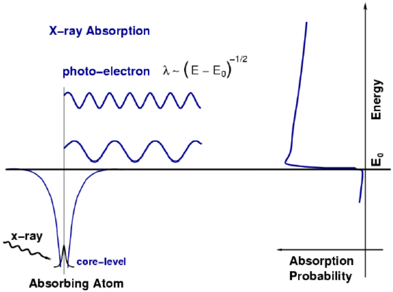

An empty final state is required.
No available state,
no absorption!
When the incident x-ray energy is larger than the binding energy, there is a sharp increase in absorption.

For an isolated atom, $\mu(E)$ has a sharp step at the core-level binding energy and is a smooth function of energy above the edge.

Image from Matt Newville

X-ray absorption in condensed matter

The ejected photo-electron can scatter from neighboring atoms. R has some relationship to λ and there is a phase shift associated with the scattering event. Thus the outgoing and scattered waves interfere.

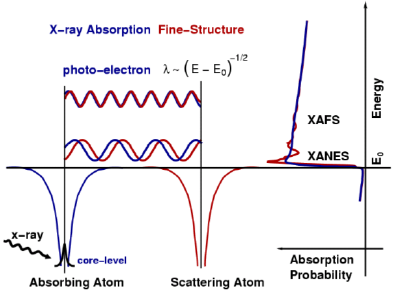

The scattering of the photo-electron wave function interferes with itself.

$\mu(E)$ depends on the density of states with energy $(E - E_0)$ at the absorbing atom.

This interference at the absorbing atom will vary with energy, causing the oscillations in $\mu(E)$.

Image from Matt Newville

The EXAFS equation

For each kind of path, we evaluate the EXAFS equation:

$$\chi(k,\Gamma) = \frac{(N_\Gamma S_0^2) F_\Gamma(k) e^{-2\sigma_\Gamma^2 k^2} e^{-2R_\Gamma/\lambda(k)}}{2\, kR_\Gamma^2} \sin\left(2kR_\Gamma + \Phi_\Gamma(k)\right) \qquad (1)$$

$$\chi_{\text{theory}}(k) = \sum_\Gamma \chi(k,\Gamma) \qquad (2)$$

$$R_\Gamma = R_{0,\Gamma} + \Delta R_\Gamma \qquad (3)$$

$$k = \sqrt{2m_e(E_0 - \Delta E_0)/\hbar^2} \approx \sqrt{(E_0 - \Delta E_0)/3.81} \qquad (4)$$

The terms in blue come from theory. (I use a thing called FEFF). FEFF treats SS and MS paths **equivalently**. F_Γ and ϕ_Γ are the *effective* scattering amplitude and phase shift for the path.

The strategy of EXAFS analysis

In IFEFFIT the terms in red are not themselves the fitting parameters. They are **written in terms of** the actual fitting parameters.

Real space multiple scattering in pictures

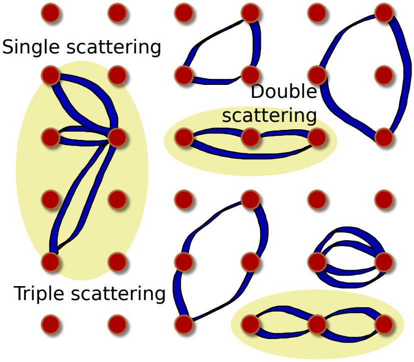

Here are some examples (in two dimensions) of single, double, and triple scattering paths.

For SS, FEFF computes the three SS paths shown and all others (up to some maximum length).

SS and *collinear* MS paths tend to be the dominant contributions to the EXAFS.

The trick to EXAFS analysis

Somehow evaluate each path and choose which ones to include in a fit.

Real space multiple scattering in pictures

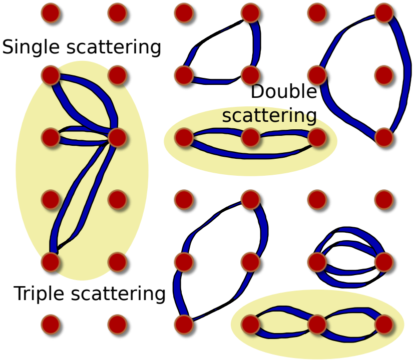

Here are some examples (in two dimensions) of single, double, and triple scattering paths.

For SS, FEFF computes the three SS paths shown and all others (up to some maximum length).

SS and *collinear* MS paths tend to be the dominant contributions to the EXAFS.

The trick to EXAFS analysis

Somehow evaluate each path and choose which ones to include in a fit.

FeS_2 structure

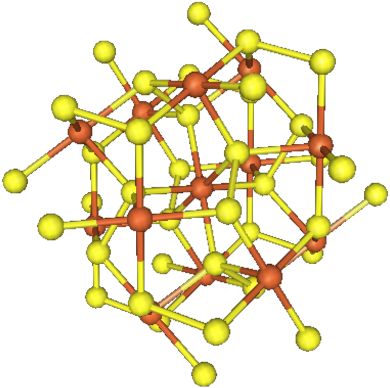

The Fe atom is surrounded by an octahedron of S atoms

- 6 S nearest neighbors at 2.257 Å
- 6 S next nearest neighbors at 3.445 Å
- 2 S scatterers at 3.594 Å
- 12 Fe scatterers at 4.167 Å

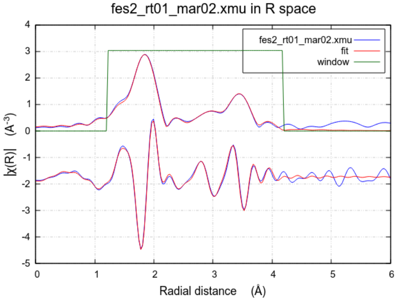

Somehow add up the contributions from each of the scatterers **and** from all the MS paths involving those scatterers.

Path expansion

$$\chi(k,\Gamma) = \frac{(N_\Gamma S_0^2) F_\Gamma(k) e^{-2\sigma_\Gamma^2 k^2} e^{-2R_\Gamma/\lambda(k)}}{2\,kR_\Gamma^2} \sin\left(2kR_\Gamma + \Phi_\Gamma(k)\right) \tag{1}$$

$$\chi_{\mathrm{theory}}(k) = \sum_\Gamma \chi(k,\Gamma) \tag{2}$$

$$R_\Gamma = R_{0,\Gamma} + \Delta R_\Gamma \tag{3}$$

$$k = \sqrt{2m_e(E_0 - \Delta E_0)/\hbar^2} \approx \sqrt{(E_0 - \Delta E_0)/3.81} \tag{4}$$

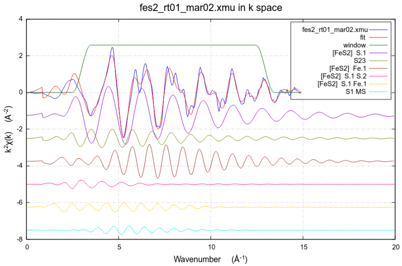

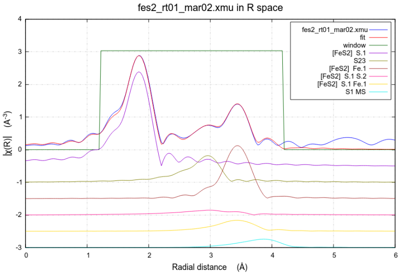

Path expansion

$$\chi(k,\Gamma) = \frac{(N_\Gamma S_0^2) F_\Gamma(k) e^{-2\sigma_\Gamma^2 k^2} e^{-2R_\Gamma/\lambda(k)}}{2\,kR_\Gamma^2} \sin\left(2kR_\Gamma + \Phi_\Gamma(k)\right) \quad (1)$$

$$\chi_{\text{theory}}(k) = \sum_\Gamma \chi(k,\Gamma) \quad (2)$$

$$R_\Gamma = R_{0,\Gamma} + \Delta R_\Gamma \quad (3)$$

$$k = \sqrt{2m_e(E_0 - \Delta E_0)/\hbar^2} \approx \sqrt{(E_0 - \Delta E_0)/3.81} \quad (4)$$

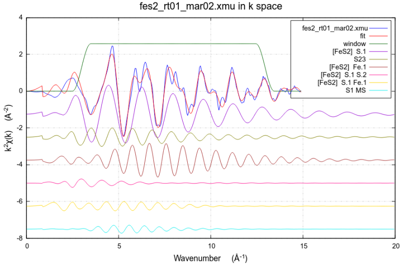

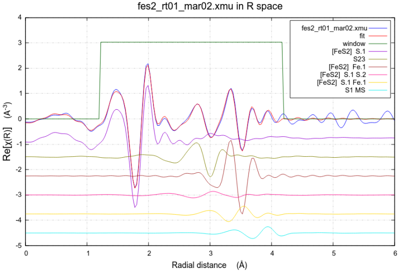

Minerology (I)

A deep understanding of the nuclear fuel cycle requires study of “exotic” pentavalent uranium minerals that can form under specific mine or storage facility conditions. One such mineral, $U^{V}(H_2O)_2(U^{VI}O_2)_2O_4(OH)+4{\cdot}H_2O$, has recently been synthesized.

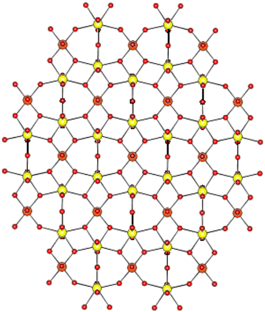

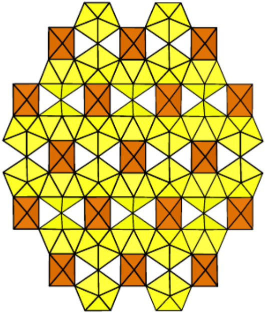

XRD is an indirect measure of valence — XAS is a direct measure!

N. Belai et el., *Pentavalent Uranium Oxide via Reduction of $[UO_2]^{2+}$ Under Hydrothermal Reaction Conditions*, Inorg. Chem., 2008, 47 (21), pp 10135-10140, DOI: 10.1021/ic801534m

Minerology (II)

XAS on $U^{V}(H_2O)_2(U^{VI}O_2)_2O_4(OH)+4\cdot H_2O$

XANES data

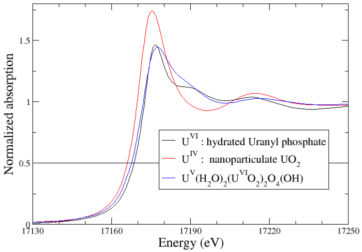

We see evidence of U^{V} by the intermediate edge position between our U^{IV} and U^{VI} standards.

EXAFS analysis

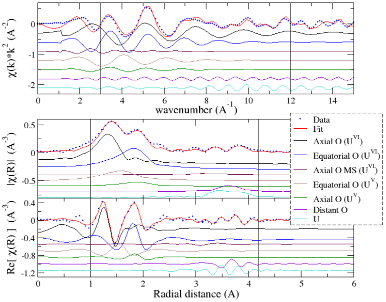

The crystal structure refined from the XRD is consistent with the EXAFS data.

N. Belai et el., *Pentavalent Uranium Oxide via Reduction of $[UO_2]^{2+}$ Under Hydrothermal Reaction Conditions*, Inorg. Chem., 2008, 47 (21), pp 10135-10140, DOI: 10.1021/ic801534m

Dielectric materials (I)

Tantalum oxynitrides are a class of dielectric materials with high K which is tunable by selection of the A cation. By mixing A cations, a temperature-constant dielectric is possible.

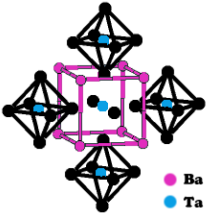

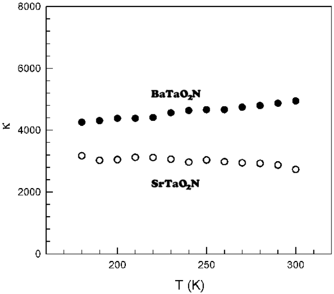

First principles DFT on $BaTaO_2N$ suggests that the different ionic radii of O and N introduce substantial disorder around the Ta atom.

B. Ravel et al., *Role of local disorder in the dielectric response of $BaTaO_2N$*, Phys. Rev. **B73**, p. 184121 (2006),
DOI: 10.1103/PhysRevB.73.184121

Dielectric materials (II)

The DFT results in a rather complex coordination environment about the Ta atom — much more complex than the simple perovskite structure.

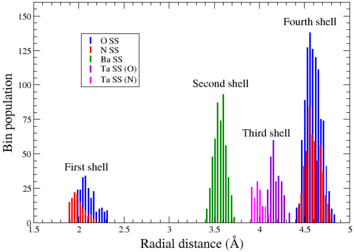

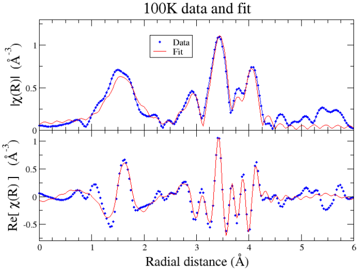

With some effort, this complexity can be incorporated into the data analysis. The EXAFS data are shown to be (mostly) consistent with the DFT results.

B. Ravel et al., *Role of local disorder in the dielectric response of* $BaTaO_2N$, Phys. Rev. **B73**, p. 184121 (2006),
DOI: 10.1103/PhysRevB.73.184121

EXAFS analysis can be quite elaborate...

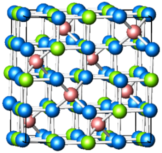

Oxygen
Octahedral site
Tetrahedral site

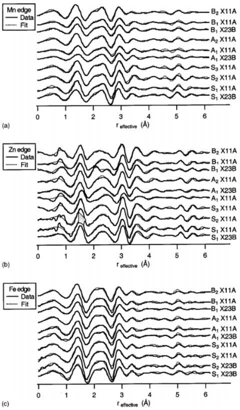

- Manganese zinc ferrite nanoparticles
- Each element can occupy each either metal site
- Oxygen vacancies can exist
- Data collected at 3 edges and on various sample preparations
- A fitting model was created using all the data simultaneously and considering occupancies of each metal on each site, oxygen vacancy, and nanoparticle undercoordination

S. Calvin et el., *Multiedge refinement of extended x-ray-absorption fine structure of manganese zinc ferrite nanoparticles*, Phys. Rev. B **66**(22) p. 224405. (2002), DOI: 10.1103/PhysRevB.66.224405
Ferrite image from `http://wikis.lib.ncsu.edu/index.php/Image:Size21.png`

Part 4

A real-world example

My vegetable garden

When I bought my house, there was a wooden deck off the dining room. I replaced this with a paving stone patio and converted the adjacent plot of ground into a vegetable garden.

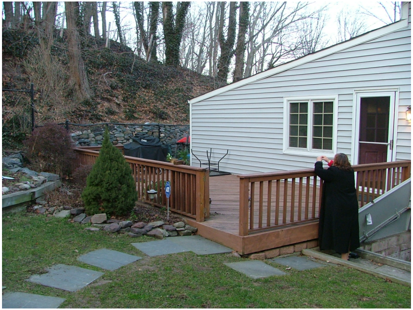

Wood preservative

The wood used to make the deck was treated with the wood preservative chromated copper arsentate (CCA), which is chromium-bearing analogue of copper orthoarsente, $Cu_3(AsO_4)_2{\cdot}4H_2O$.

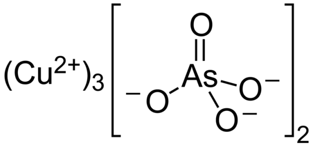

CCA-treated wood is known to leach all three elements into surrounding soils. I had some questions:

1. How much As is in the soil? Is it higher near the patio than elsewhere in the garden? (Use XRF)
2. What chemical species is the As in the soil? (Use XAS)

The orthoarsenate image is from Wikimedia commons and is in the public domain.

XRF spectra

I took soil samples from a few centimeters below the surface from a spot adjecent to the old deck and from a spot 5 meters away and slightly uphill.

Here are the XRF spectra from those two spots:

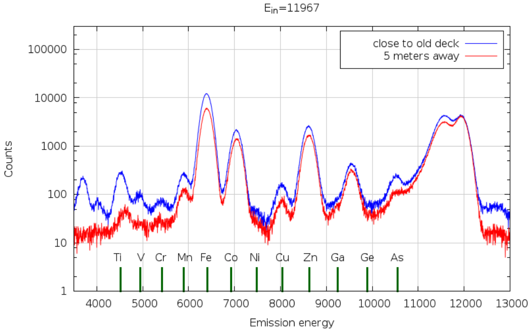

There is a clear enhancement of both As and Cr in the soil adjacent to the old deck. The As is enhanced roughly two-fold.

As standards

As a point of reference, here are the XAS spectra from two inorganic As standards, $As_2^{3+}O_3$ and $As_2^{5+}O_5$.

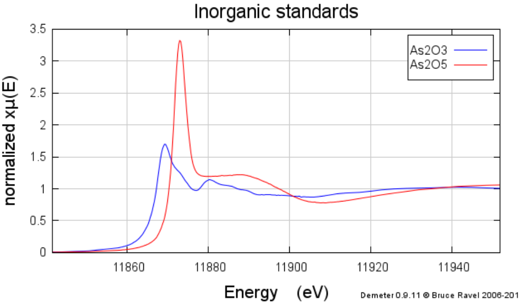

Note that the edge of As^{5+} standard is shifted substantially to higher energy and that the first peak is much enhanced.

As^{5+} is water soluble, thus more mobile than As^{3+}.
Also As^{5+} is quite toxic.

XAS from the soil samples

Here are the raw $\mu(E)$ data from the two soil locations. Sure enough, the signal from the site adjacent to the old deck is enhanced by about a factor of 2.

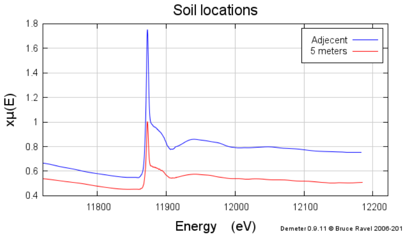

Should I be worried about eating produce from my garden?

XAS from the soil samples

Here are the raw $\mu(E)$ data from the two soil locations. Sure enough, the signal from the site adjacent to the old deck is enhanced by about a factor of 2.

Here are the normalized data compared to standards. The As is slightly reduced, but predominantly As^{5+}. As in soil is well known to bind to soil particles as As^{5+}.

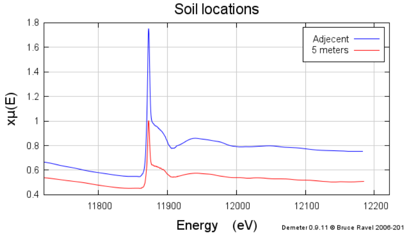

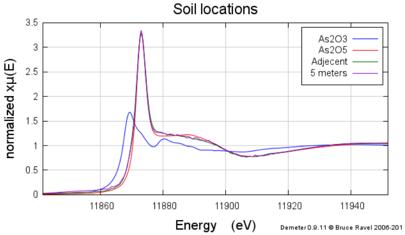

Should I be worried about eating produce from my garden?

XAS from the soil samples

Here are the raw $\mu(E)$ data from the two soil locations. Sure enough, the signal from the site adjacent to the old deck is enhanced by about a factor of 2.

Here are the normalized data compared to standards. The As is slightly reduced, but predominantly As^{5+}. As in soil is well known to bind to soil particles as As^{5+}.

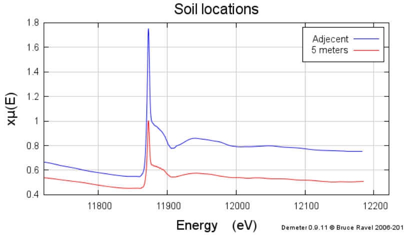

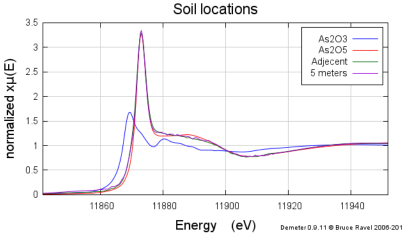

Should I be worried about eating produce from my garden?

XRF spectra from plant leaves

Here are XRF spectra from the leaf of a squash plant growing in the soil adjacent to the old deck.

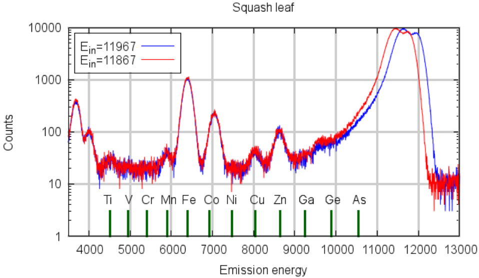

Although toxic As^{5+} is present in the soil in elevated quantities, very little is taken up by the plants growing that soil.

XRF spectra from plant leaves

Here are XRF spectra from the leaf of a squash plant growing in the soil adjacent to the old deck.

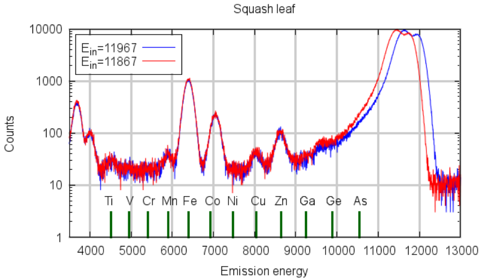

Although toxic As^{5+} is present in the soil in elevated quantities, very little is taken up by the plants growing that soil.

The squash were delicious!

More information

About NSLS-II

- http://www.bnl.gov/nsls2

About synchrotron science

- http://www.lightsources.org/

About X-ray Absorption Spectroscopy

- http://www.xrayabsorption.org/
- XAFS for Everyone by Scott Calvin

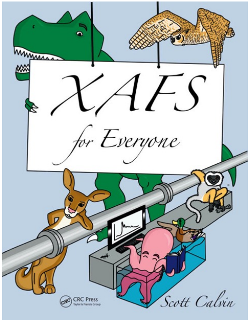

Information about XAS

http://xrayabsorption.org/Tutorials

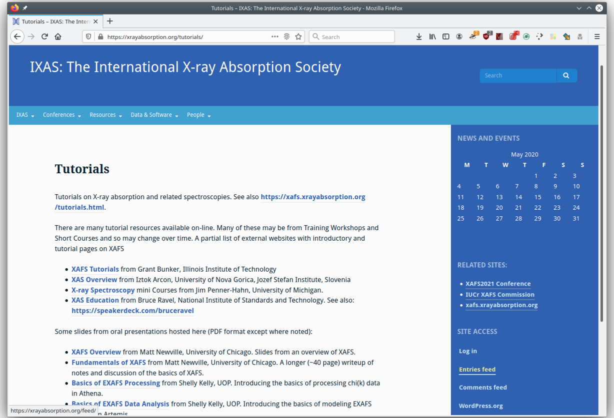

Free* XAS software

http://bruceravel.github.io/demeter/

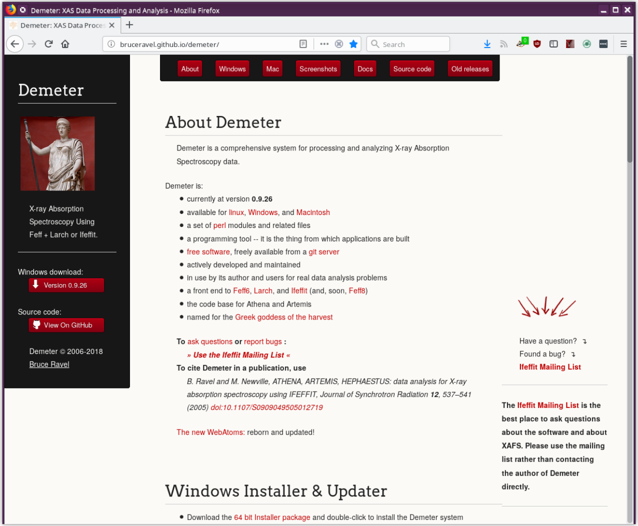

* **Free** of cost, **freely** available source code, **freely** redistributable